Talanta 93 (2012) 350–357

Contents lists available at SciVerse ScienceDirect

Talanta

journal homepage: www.elsevier.com/locate/talanta

# Preparation and characterization of chitosan/graphene oxide composites for the adsorption of Au(III) and Pd(II)

Li Liu, Cui Li, Changli Bao*, Qiong Jia, Pengfei Xiao, Xiaoting Liu, Qiuping Zhang

*College of Chemistry, Jilin University, 130026 Changchun, PR China*

ARTICLE INFO

*Article history:*
Received 2 November 2011
Received in revised form 16 February 2012
Accepted 22 February 2012
Available online 1 March 2012

*Keywords:*
Chitosan
Graphene oxide
Composite
Preparation
Adsorption

ABSTRACT

In this work, graphene oxide (GO) was firstly prepared, following by element analysis. Glutaraldehyde cross-linked chitosan (GCCS) and chitosan/graphene oxide (CSGO) composite with three different amounts of GO (5 wt%, 10 wt% and 15 wt%) were also prepared for the adsorption of Au(III) and Pd(II) in aqueous solution. The properties of the adsorbents were investigated by Fourier transform infrared spectroscopy (FT-IR), X-ray diffraction (XRD) and surface area analysis. Batch adsorption studies were carried out. The adsorption of Au(III) and Pd(II) onto CSGO composites was optimum at pH 3.0–5.0 for Au(III) and pH 3.0–4.0 for Pd(II), which was much wider than that of GCCS. The adsorption isotherms obeyed the Langmuir isotherm models for the adsorption of Au(III) and Pd(II). Chitosan with 5 wt% graphene oxide ($CSGO_5$) composite had the largest adsorption capacity for Au(III) and Pd(II) compared with the other prepared adsorbents, where the maximum adsorption capacity were 1076.649 mg/g for Au(III) and 216.920 mg/g for Pd(II), respectively. The adsorption kinetics of Au(III) and Pd(II) onto $CSGO_5$ followed a pseudo-second-order kinetic model, indicating that the chemical adsorption was the rate-limiting step. Thermodynamic parameters, such as Gibbs energy ($\Delta G^\circ$), enthalpy ($\Delta H^\circ$), and entropy ($\Delta S^\circ$), were calculated, showing that the adsorption of Au(III) and Pd(II) onto $CSGO_5$ were spontaneous, endothermic and feasible. The desorption studies of Au(III) and Pd(II) onto $CSGO_5$ showed that $CSGO_5$ can be used repeatedly without significantly changing its adsorption capacity and desorption percentage after 3 cycles. Besides $CSGO_5$ was successfully applied for the determination and separation of Au(III) and Pd(II) in ore samples.

## 1. Introduction

Due to the specific physical and chemical properties of precious metals, they are widely used in many fields, such as jewelery, biomedicine, aerospace construction, agriculture and catalysts in various chemical processes [1]. Therefore more and more attention has been gained for the recovery of these metals from aqueous solutions. There are many processes of separating and enriching metal ions from aqueous solutions, such as ion-exchange [2], coprecipitation [3,4], extraction [5,6], membrane filtration [7,8], electrolysis [9] and adsorption [10,11]. Among all of the methods, the adsorption seems to be a more suitable method for the adsorption of precious metals due to low cost, simply operating, no or little use of organic solvents, and high efficiency. In addition, researches of alternative adsorbents remain a priority in the field of adsorption method. From the view of environment and economy, biosorbents attract a strong interest as a more environmental and cost effective alternative, such as lignin [12,13], activated carbon [14–16], bone gelatin [17] and kenaf [18].

Among biosorbents, chitosan (CS), the linear cationic aminopolysaccharide composed of α-D-glucosamine, is a partially acetylated glucosamine biosorbent and extracted by a deacetylation procedure from chitin, the most abundant biopolymer in nature after cellulose [19,20]. Recent years, the application of chitosan has been attracted numerous scientists. Due to the outstanding properties of chitosan, such as nontoxic, biocompatibility, hydrophilic, antibacterial activity [21], it has been extensively used in various fields, such as biomaterials [22,23], textile [24], drug delivery [25], environmental protection [26], and metallurgy [27,28]. The amine and two hydroxyl groups on each glucosamine monomer act as adsorption sites, especially the amine groups which are strongly reactive with metal ions. However, the applications of chitosan are limited because of its solubility in acid solution. Hence, it is necessary to crosslink chitosan in order to make it stable in acid solution. The cross-linking procedure

---

* Corresponding author at: Ximinzhu Street 6#, Changchun 130026, PR China. Tel.: +86 431 88502259.
*E-mail address:* baocl@jlu.edu.cn (C. Bao).

0039-9140/$ – see front matter © 2012 Elsevier B.V. All rights reserved.
doi:10.1016/j.talanta.2012.02.051

of chitosan is made between functional groups of chitosan and different kinds of cross-linking agents, such as glutaraldehyde [29], and epichlorohydrin [30].

Besides biosorbents, graphene which can be prepared from the low cost material graphite, is intensively investigated as adsorbents for metal ions [31]. Since the discovery of graphene, more and more attention is focused to develop the application of the properties of graphene and its derivatives, because of their unique structure, extraordinary electronic, mechanical properties and high thermal conductivity [32,33]. Graphene oxide (GO), which is one of the graphene derivatives, has gained considerable attention as a significant adsorbent [34]. There are plenty of oxygen atoms on the graphitic backbone of GO in the forms of epoxy, hydroxyl, and carboxyl groups, which protrude from its layers. These groups can bind to metal ions well. In addition, the huge surface area of GO makes it have a large adsorption capacity which is similar to carbon nanotube adsorption [35].

In the present study, graphene oxide (GO), glutaraldehyde cross-linked chitosan (GCCS) and chitosan/graphene oxide (CSGO) composites were prepared and characterized. The purpose of this study is to prepare CSGO composites with enhanced adsorption capacity for Au(III) and Pd(II). And the experimental studies were carried out by batch adsorption studies. Various parameters such as pH, initial concentration, contact time, adsorption isotherms and kinetics, effect of temperature, and desorption were studied. Moreover, the standard ore samples were carried out to check up the feasibility of $CSGO_5$.

## 2. Experimental

### 2.1. Materials and reagents

Chitosan, with a deacetylation degree of about 90%, was purchased from Boao Biological Tech. Co. Ltd in China. Graphite powder, analytical grade, was obtained from Tianjin Guangfu Fine Chemical Research Institute. The other reagents, such as HAc, NaOH, 98% $H_2SO_4$, $H_2O_2$, HCl, $KMnO_4$, glutaraldehyde and isopropyl alcohol, were supplied by Beijing Chemical Reagent Factory. Atomic adsorption spectrometry standard solutions of 1000 mg/L Au(III) and 1000 mg/L Pd(II) were from Beijing NCS Analytical Instruments Co. Ltd. Working standards were stepwise diluted by the standard solutions every time. All of the chemicals used in this study were of analytical grade. Solutions were diluted by using ultrapure water.

### 2.2. Instrumentation and methods of characterization

The concentrations of Au(III) and Pd(II) were analyzed by the TAS-990 flam atomic adsorption spectrophotometer (PGeneral, China).

The contents of C and H elements in GO were performed on a vario microorganic elemental analyzer (Elementar Co., Germany).

An Affinity-1 Fourier transform infrared spectrophotometer (Shimadzu, Japan) was used to analyze the functional groups. KBr pellets were used and the resolution was 4 $cm^{-1}$ with 64-time scanning, and the scanning was performed in the range of 4000–400 $cm^{-1}$.

The X-ray diffraction (XRD) measurements of GCCS, GO and CSGO composites were recorded using Shimadzu 6000 X-ray diffractometer (Shimadzu, Japan) with a detector operating under a voltage of 40.0 kV and a current of 30.0 mA using Cu Kα radiation ($\lambda = 0.15418$ nm). The recorded range of $2\theta$ was 4–70°, and the scanning speed was 6°/min.

The surface area was investigated by SSA-3600 intelligent surface area analyzer (Builder Technology Co. Ltd, China) by $N_2$ physisorption.

### 2.3. Preparation of graphene oxide (GO)

Purified natural graphite was used to prepare GO according to the well-known Hummer's method with some modification [36,37]. In brief, 1.0 g graphite powder and 23 mL 98% $H_2SO_4$ were put into a 250 mL flask. The mixture was kept at an ice-water bath in order to keep the temperature below 20°C under stirring until the graphite dispersed absolutely. Successively, 3 g $KMnO_4$ power was added into the solution by batch addition. After the addition, the mixture was sequentially kept at an ice water batch for 20 min under stirring. Then the flask was kept at 35°C for 2 h. 46 mL ultrapure water was added into the flask and the temperature rose up to 90°C quickly. After 140 mL ultrapure water was added quickly, 2.5 mL $H_2O_2$ was put into the mixture. A lot of bubbles produced and the color of the solution became yellow from black. Then the mixture was filtered and washed with 5 wt% HCl solution for 4 times and ultrapure water for 5 times to remove the residual acid. The oxidation product was dialyzed by ultrapure water for one week. In the dialyzing process, the water was changed every 2 h in the former 3 times and then every 24 h once. Then the products were centrifuged at 10,000 rpm for 2 h. Finally, the product was dried at 60 °C.

### 2.4. Preparation of CSGO composites

The prepared GO was easily dispersed into 20 mL 1% (v/v) acetic acid solution. Then it was treated by ultrasound for 30 min at room temperature and formed a homogeneous suspension. 0.5 g chitosan powder was added into the suspension respectively under stirring and then it was treated by ultrasound for another 1 h in order to make chitosan dissolve absolutely and mix with GO uniformly. After rested for 12 h, the well-distributed suspension was dropped into 3.0% (w/v) aqueous sodium hydroxide solution, by using a 0.05-mm diameter injector and the injection speed was about 60 drops 1 min. 24 h later, the beads became solidified and were washed several times by ultrapure water until the pH value of the water was nearly neutral. Then the beads were filtered and put into a 250 mL flask. 30 mL methanol and 1.5 mL 50% aqueous solution of glutaraldehyde were added into it, successively. Then they were stirred at room temperature for 5 h. Finally, the beads were isolated by filtration and washed several times by ethanol and followed by ultrapure water.

By changing the weight of GO into 0.5 g chitosan, such as 0.0263:0.5, 0.0556:0.5 and 0.0882:0.5, a series of chitosan/graphene oxide composites coded as $CSGO_5$, $CSGO_{10}$, $CSGO_{15}$ were prepared, respectively. It is obvious that the weight percentage of GO in the composites are 5 wt%, 10 wt% and 15 wt%. In addition, the glutaraldehyde cross-linked chitosan without GO, coded as GCCS, was also prepared according to the same method.

### 2.5. Adsorption studies

Batch adsorption studies were conducted by placing a certain amount of adsorbents into metal ion solutions with different concentrations at room temperature. The solution pH was adjusted to the desired value with HCl and the concentration of metal ions was determined by FAAS. The adsorption capacity was calculated by Eq. (1)

$$q = \frac{(C_0 - C_e)}{m} V \qquad (1)$$

where $q$ (mg/g) is the adsorption capacity of the adsorbent, $C_0$ and $C_e$ (mg/L) are the initial and final concentrations of metal ion in solutions, respectively. $V$ (L) is the volume of the aqueous solutions and $m$ (g) is the mass of the adsorbent.

### 2.6. *Effect of temperature*

The effect of temperature on the adsorption of Au(III) and Pd(II) onto $CSGO_5$ was investigated at 303 K, 313 K and 323 K.

### 2.7. *Desorption studies and reuse*

The desorption studies of the adsorbed metal ions from $CSGO_5$ was carried out by HCl, thiourea and thiourea–HCl solutions. The desorption percentage was calculated with Eq. (2)

$$\text{Desorption}\,(\%) = \frac{C_e{}'V}{qm} \times 100\% \tag{2}$$

where $q$ (mg/g) is the adsorption capacity of the adsorbent. $m$ (g) is the mass of the adsorbents and $V$ (L) is the volume of the aqueous solutions. $C_e{}'$ (mg/L) is the concentrations of Au(III) and Pd(II) aqueous solutions after completely desorbed from the adsorbent.

### 2.8. *Sample analysis*

The standard ore sample of GBW(E)070015 (10.00 μg/g Au) and GBW07293 (0.568 μg/g Pd) were placed in porcelain crucible, heated for 3 h at 600 °C in a baffle furnace and then cooled. Then the sample was pretreated with aqua regia for about 1 h. The solutions were evaporated to moist salt state. The final residue was dissolved in 5 mL concentrated HCl, filtered, transferred into a 50 mL color comparison tube and diluted to volume with deionized water, successively. The released metal ions in the solution were determined by flam atomic adsorption spectrophotometer.

## 3. Results and discussion

### 3.1. *Characterization*

The element analysis of GO result showed that GO had a composition of 47.665% carbon, 2.588% hydrogen (by weight). And the weight percentage of oxygen was calculated nearly 50%. The results indicated that the oxidation process was perfect, which was favorable for the adsorption of metal ions.

Chitosan, GO, CSGO composites and CSGO-metal ions were characterized by FT-IR and the results are shown in Fig. 1 and Table 1. The FT-IR spectrum of GO (curve b) was similar to a previous report in the literature [38,39], as well as the FT-IR spectrum of chitosan (curve a) [28]. The peaks of CSGO (curve c) showed a similar to that of chitosan and GO. The peak at 1665 $cm^{-1}$ and 1591 $cm^{-1}$ were assigned to the COOH groups and the C═C groups from GO, respectively. Both of the two peaks were downshifted compared to GO, due to the hydrogen bonding between chitosan and GO. The results implied the existence of the interaction between chitosan and GO. Finally, the FT-IR spectrum results of CSGO-metal ions are shown in Fig. 1B indicated that the intensity of the peaks at about 3430 $cm^{-1}$, 1659 $cm^{-1}$ and 1591 $cm^{-1}$ changed and even some peaks disappeared compared to the peaks of CSGO, which might suggest the chemical reaction between previous metals and the functional groups, such as $NH_2$, OH, COOH, and C═C groups. Besides, as shown in Table 1, some peaks such as 1665 $cm^{-1}$, 1156 $cm^{-1}$, 1018 $cm^{-1}$, 1070 $cm^{-1}$ were shifted after the adsorption, also signifying the feasible participation of the functional groups on CSGO composites.

The XRD patterns of GO, GCCS and CSGO composites were shown in Fig. 2. The characteristic XRD peak of GO appeared at $2\theta = 11.3^\circ$ [40]. All of GCCS and CSGO composites exhibited a broad peak at $2\theta = 20.3^\circ$ due to the amorphous state of the chitosan. Apparently, the diffraction peaks of the CSGO composites were similar to GCCS and the diffraction peaks of GO were not seen in the XRD peak of CSGO composites, indicating that the amorphous structure of

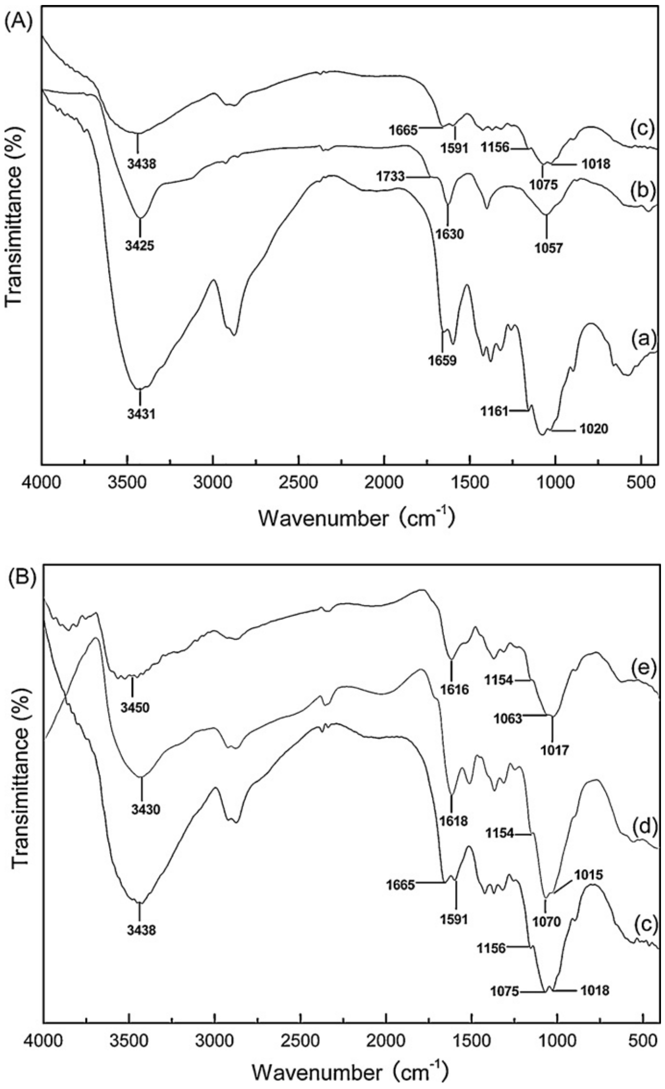

**Fig. 1.** FT-IR spectra: (A) chitosan (curve a), GO (curve b) and CSGO (curve c); (B) CSGO (curve c), CSGO-Au(III) (curve d) and CSGO-Pd(II) (curve e).

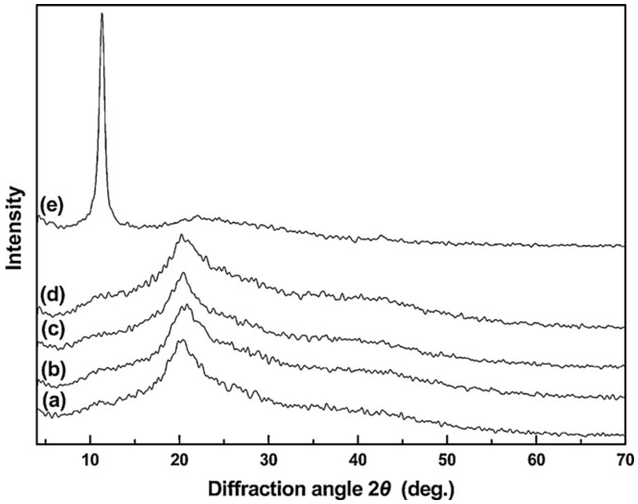

**Fig. 2.** XRD patterns: (a) GCCS, (b) $CSGO_5$, (c) $CSGO_{10}$, (d) $CSGO_{15}$ and (e) GO.

**Table 1**
Characteristic IR-band of chitosan, GO and CSGO.

| Assignment | Wavenumber ($cm^{-1}$) | | | | |
|---|---|---|---|---|---|
| | Chitosan [28] | GO [38,39] | CSGO | CSGO-Au(III) | CSGO-Pd(II) |
| $\upsilon_{N-H(NH)_2}$, $\nu_{N—H(amide)}$ | 3431 | – | 3438 | 3430 | 3450 |
| $\nu_{C=O(amide)}$ | 1659 | – | 1665 | 1618 | 1616 |
| $\nu_{C—O(primary\ alcoholic\ groups\ of\ C6—OH)}$ | 1161 | – | 1156 | 1154 | 1154 |
| $\nu_{C—O(secondary\ alcoholic\ groups\ of\ C3—OH)}$ | 1020 | – | 1018 | 1015 | 1017 |
| $\nu_{O—H}$ | 3431 | 3425 | 3438 | 3430 | 3450 |
| $\nu_{C=O(COOH)}$, $\nu_{C=O(carbonyl)}$ | – | 1733 | 1665 | 1618 | 1616 |
| $\nu_{C=C}$ | – | 1630 | 1591 | – | – |
| $\nu_{C—O(epoxy)}$, $\nu_{C—O(alkoxy)}$ | – | 1057 | 1075 | 1070 | 1063 |

GCCS was not changed by the addition of GO and GO was well exfoliated with chitosan in CSGO composites. Thus, there might be mainly physical interaction (hydrogen bonding) but scarcely chemical reaction between chitosan and GO. Besides, the diffraction intensity of GCCS was a little stronger than that of CSGO composites at $2\theta = 20.3°$, implying that the crystalline degree of chitosan decreased after adding GO into chitosan.

The surface areas were calculated to be 1.560 $m^2$/g, 4.232 $m^2$/g, 7.643 $m^2$/g and 9.406 $m^2$/g for GCCS, $CSGO_5$, $CSGO_{10}$ and $CSGO_{15}$, respectively. It is clear that with the addition of GO, the surface areas of CSGO composites became larger than that of GCCS, resulting that the CSGO composites might be able to enhance the adsorption capacity of Au(III) and Pd(II).

### 3.2. *Effect of pH*

The effect of pH ranging from 1.0 to 6.0 for the adsorption of Au(III) and Pd(II), at equilibrium and on three adsorbents of CSGO composites ($CSGO_5$, $CSGO_{10}$ and $CSGO_{15}$) was studied and the initial concentration of Au(III) and Pd(II) were 80 mg/L and 40 mg/L, respectively. The desired pH was adjusted using HCl. The results indicated that the adsorption capacity of Au(III) and Pd(II) increased with increasing pH values and then decreased at higher pH values from 5.0 to 6.0, since the hydrolyzed chlorogold complex and $Pd(OH)_2$ may be formed which is precipitated and make the Au(III) and Pd(II) ions unavailable for the adsorption process. The maximum adsorption amounts on CSGO composites were obtained in the range of 3.0–5.0 in case of Au(III) and 3.0–4.0 in case of Pd(II). The effect of pH was also studied on GCCS and GO. The adsorption capacity reached to maximum when pH was 4.0 and 3.0 in case of GCCS and pH was both 5.0 in case of GO for Au(III) and Pd(II), respectively.

The adsorption mechanisms of Au(III) and Pd(II) with GCCS may be mainly the ion interaction between protonated amines and tetrachloro-aurate, chloro-palladate complexes, and the coordination of Au(III) and Pd(II) with nitrogen atoms and oxygen atoms. In acid solutions, the amine groups are easily protonated. The $pK_a$ of chitosan ranges from 6.3 to 7.2 [40] and at pH 4 the amine groups are almost 100% protonated. Hence, protonated amine groups may cause electrostatic interaction of anionic metal complexes which result from metal chelation by chloride ligands in this study. What's more, nitrogen atoms and oxygen atoms hold free electron doublets that may react with metals.

With the addition of GO into chitosan, the maximum adsorption amounts on CSGO composites occurred at a wider pH range than that of GCCS. The reason may be that at lower pH values, the amine groups of chitosan are the mainly effective adsorptive groups, reacting with metal ions. While at higher pH values, the nitrogen and oxygen atoms of chitosan, as well as a plenty of oxygen atoms on GO might coordinate with metals. Besides, there might be weak adsorption between metals and Cπ electrons on GO layer.

In the following adsorption experiments, pH 4.0 for Au(III) and pH 3.0 for Pd(II) were chosen in case of GCCS and CSGO composites, while pH 5.0 for Au(III) and Pd(II) were used in case of GO.

### 3.3. *Adsorption isotherms*

Batch adsorption experiments were conducted. Then 10 mL solutions with various initial concentrations (80–500 mg/L for Au(III) and 10–100 mg/L for Pd(II) in case of GCCS and CSGO composites while 10–100 mg/L in case of Au(III) and 10–100 mg/L in case of Pd(II) in case of GO) were shaken for 16 h at room temperature with 2 mg GO, 2 mg CSGO composites and 2 mg GCCS, respectively. And the solution pH was adjusted to the desired value by using HCl. In order to interpret the adsorption experimental data, the most frequently used equations are the Langmuir [41] and Freundlich [42] isotherm equations.

The Langmuir isotherm assumes monolayer adsorption and the adsorption occurs at specific homogeneous adsorption sites. The expression of the Langmuir isotherm equation is expressed by Eq. (3)

$$q_e = \frac{q_m b C_e}{1 + b C_e} \tag{3}$$

where $q_e$ (mg/g) is the adsorption capacity of Au(III) and Pd(II) at equilibrium, $q_m$ (mg/g) is the theoretical saturation adsorption capacity for monolayer coverage, $C_e$ (mg/L) is the concentration of Au(III) and Pd(II) at equilibrium, and $b$ (1/mg) is the Langmuir constant related to the affinity of binding sites and is a measure of the energy of adsorption. These constants can be calculated from the slop and intercept of the linear plot of $C_e/q_e$ vs. $C_e$. In addition, the parameter $R_L$, called the equilibrium parameter, is calculated as Eq. (4) to identify whether an adsorption system is favorable or unfavorable.

$$R_L = \frac{1}{1 + b C_0} \tag{4}$$

where $C_0$ (mg/g) is the initial concentration. If $R_L > 1$, the adsorption process is favorable; if $R_L = 1$, the process is linear; if $R_L < 1$, the process is unfavorable and if $R_L = 0$, the process is irreversible.

Different from Langmuir isotherm, the Freundlich isotherm assumes heterogeneous adsorption due to the diversity of the adsorption sites or the diverse nature of the metal ions adsorbed. The Freundlich adsorption equation is given as Eq. (5)

$$q_e = k {C_e}^{1/n} \tag{5}$$

where $k$ and $n$ are the Freundlich constants, related to adsorption capacity of adsorbent and adsorption intensity, respectively. $k$ and $n$ can be obtained from the slope and intercept of the linear plot of $\log q_e$ vs. $\log C_e$.

The adsorption data of Au(III) and Pd(II) onto GO, GCCS and different CSGO composites are shown in Figs. 3 and 4. Table 2 displays the constants of Langmuir and Freundlich isotherm for the adsorption of Au(III) and Pd(II) on GO, GCCS and CSGO composites,

**Table 2**
Constants of Langmuir and Freundlich isotherms for adsorption of Au(III) and Pd(II) on GO, GCCS and GCCS,CSGO$_5$, CSGO$_{10}$ and CSGO$_{15}$.

| Metal | Adsorbent | Langmuir isotherm | | | | Freundlich isotherm | | |
|---|---|---|---|---|---|---|---|---|
| | | $q_m$ (mg/g) | $b$ (L/mg) | $R^2$ | $R_L$ | $k$ | $n$ | $R^2$ |
| Au(III) | GO | 146.199 | 0.1831 | 0.9985 | $0.0214 < R_L < 0.0639$ | 39.270 | 3.0839 | 0.9003 |
| | GCCS | 990.099 | 0.1640 | 0.9996 | $0.0238 < R_L < 0.0708$ | 434.460 | 6.4041 | 0.9604 |
| | CSGO$_5$ | 1076.649 | 0.1686 | 0.9995 | $0.0232 < R_L < 0.0690$ | 460.055 | 6.1305 | 0.9626 |
| | CSGO$_{10}$ | 925.926 | 0.1865 | 0.9998 | $0.0210 < R_L < 0.0628$ | 420.126 | 6.6401 | 0.9440 |
| | CSGO$_{15}$ | 869.565 | 0.1397 | 0.9996 | $0.0278 < R_L < 0.0821$ | 383.469 | 6.6556 | 0.9295 |
| Pd(II) | GO | 98.328 | 0.2051 | 0.9952 | $0.0191 < R_L < 0.0575$ | 29.109 | 3.2946 | 0.7154 |
| | GCCS | 180.180 | 0.5539 | 0.9998 | $0.0072 < R_L < 0.0221$ | 76.151 | 4.0640 | 0.8173 |
| | CSGO$_5$ | 216.920 | 0.7840 | 0.9996 | $0.0051 < R_L < 0.0157$ | 100.654 | 4.2960 | 0.8093 |
| | CSGO$_{10}$ | 173.010 | 0.4680 | 0.9997 | $0.0085 < R_L < 0.0260$ | 68.835 | 3.8372 | 0.8289 |
| | CSGO$_{15}$ | 160.000 | 0.5880 | 0.9997 | $0.0068 < R_L < 0.0208$ | 68.320 | 4.1384 | 0.7903 |

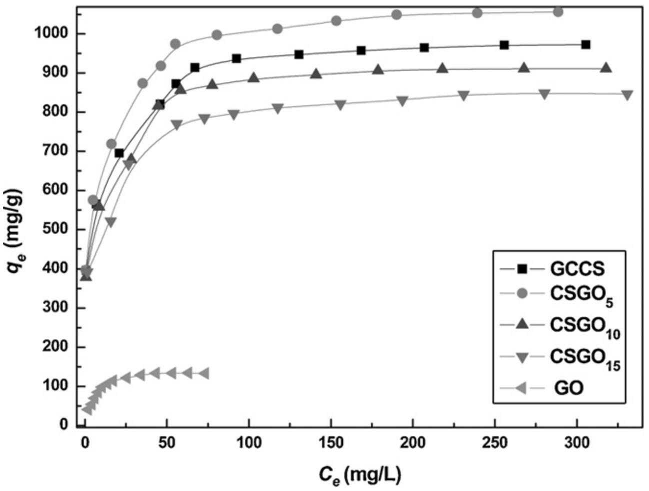

**Fig. 3.** Adsorption isotherms of Au(III) onto GO, GCCS,CSGO$_5$, CSGO$_{10}$ and CSGO$_{15}$ (adsorbent dose: 2 mg; contact time: 16 h; initial concentrations for GO: 10–100 mg/L, while for GCCS and CSGO composites: 80–500 mg/L).

respectively. It can be seen that the $R_L$ values are between 0 and 1, indicating that the adsorption are favorable. The $n$ values are between 1 and 10, suggesting that the adsorption is favorable at the studied conditions. The $R^2$ values for the Langmuir isotherm models are above 0.95 in case of Au(III) and Pd(II) indicate that the Langmuir isotherm fits the experimental data better than the Freundlich isotherm. As shown in Table 2, the maximum adsorption capacity of the monolayer ($q_m$) for Au(III) are 146.199 mg/g, 990.099 mg/g, 1076.649 mg/g, 925.926 mg/g and 869.565 mg/g on GO, GCCS, CSGO$_5$, CSGO$_{10}$, and CSGO$_{15}$, respectively. While in case of Pd(II) those are 98.328 mg/g, 180.180 mg/g, 216.920 mg/g, 173.010 mg/g and 160.000 mg/g, respectively. The results show the following order of the maximum adsorption capacity of Au(III) and Pd(II) on various adsorbents: CSGO$_5$ > GCCS > CSGO$_{10}$ > CSGO$_{15}$ > GO. The increase of the adsorption capacity of the CSGO$_5$ compared with GCCS could be explained that the increase of surface area with the addition of GO contributes to the increase of adsorption capacity, while the favorable functional groups of CSGO$_5$ decreased little than that of GCCS. The functional groups of GO maybe the carboxyl, hydroxyl, and epoxy functional groups. Besides, the Cπ electrons on GO layers may have weak adsorption for metals. While the decrease of the adsorption capacity with further increase of GO in CSGO composites may be attributed to the decrease of the chitosan content in the whole mass of the composite and chitosan is the main component due to the functional groups of chitosan, which is able to bind previous metal ions and better for the adsorption of metals than that of GO.

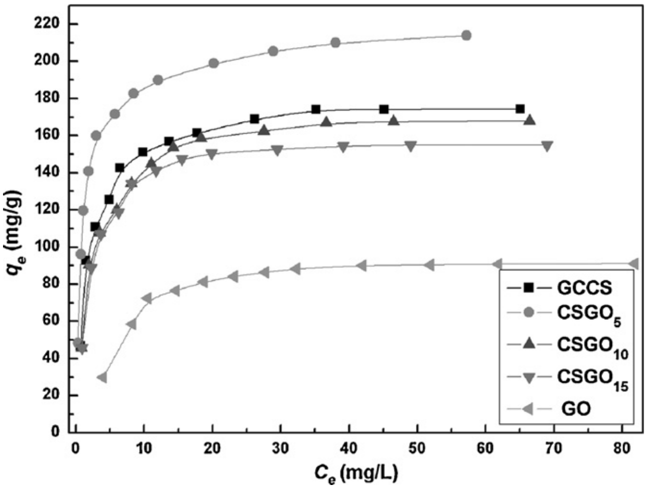

**Fig. 4.** Adsorption isotherms of Pd(III) onto GO, GCCS, CSGO$_5$, CSGO$_{10}$ and CSGO$_{15}$ (adsorbent dose: 2 mg; contact time: 16 h; initial concentrations: 10–100 mg/L).

### 3.4. Adsorption kinetics

Batch experiments about the adsorption kinetics for the adsorption of Au(III) and Pd(II) on 2 mg CSGO$_5$ were executed using the metal initial concentration of 30 mg/L for Au(III) and 20 mg/L for Pd(II) with desired pH. The contact time was 1–20 h and 1–20 h in case of Au(III) and Pd(II), respectively. Two conventional pseudo-second-order [43,44] and intraparticle diffusion [45,46] models were used to fit the experimental data in this work. The pseudo-second-order kinetic model after transformation into linear form was expressed as Eq. (6)

$$\frac{t}{q_t} = \frac{1}{k_2 {q_e}^2} + \frac{t}{q_e} \tag{6}$$

where $q_e$ and $q_t$ (mg/g) are the capacity of Au(III) and Pd(II) adsorbed at equilibrium and time $t$ (h), respectively. $k_2$ is the pseudo-second-order rate constant (g/(mg h)). Additionally, $h$ (mg/g h) stands for original adsorption rate which can be defined as $h = k_2 q_e^2$.

The adsorption kinetic data are tested whether the intraparticle diffusion is the rate-limiting step. The intraparticle diffusion kinetic model can be written as Eq. (7)

$$q_t = k_{id} t^{0.5} \tag{7}$$

where $k_{id}$ is the intraparticle diffusion rate constant, which can be obtained from the slope of the plot $q_t$ vs. $t^{0.5}$. The line of $q_t$ vs. $t^{0.5}$ suggests the applicability of intraparticle diffusion controlling the kinetics of the adsorption. If the regression of $q_t$ vs. $t^{0.5}$ is linear and passes through the origin, then intraparticle diffusion is the sole rate-limiting step. If the line does not pass through the origin,

**Table 3**
Pseudo-second-order kinetic parameters and intraparticle diffusion rate constants for the adsorption of Au(III) and Pd(II) on CSGO$_5$.

| Metal | $q_{e,exp}$ (mg/g) | Pseudo-second-order kinetic | | | | Intraparticle diffusion | |
|---|---|---|---|---|---|---|---|
| | | $k_2$ (g/mg h) | $h$ (mg/g h) | $q_{e(cal)}$ (mg/g) | $R^2$ | $k_{id}$ (mg/g h$^{0.5}$) | $R^2$ |
| Au(III) | 146.46 | 0.02315 | 523.56 | 150.38 | 0.9998 | 9.5711 | 0.7968 |
| Pd(II) | 96.04 | 0.01698 | 171.82 | 100.60 | 0.9996 | 10.8697 | 0.8329 |

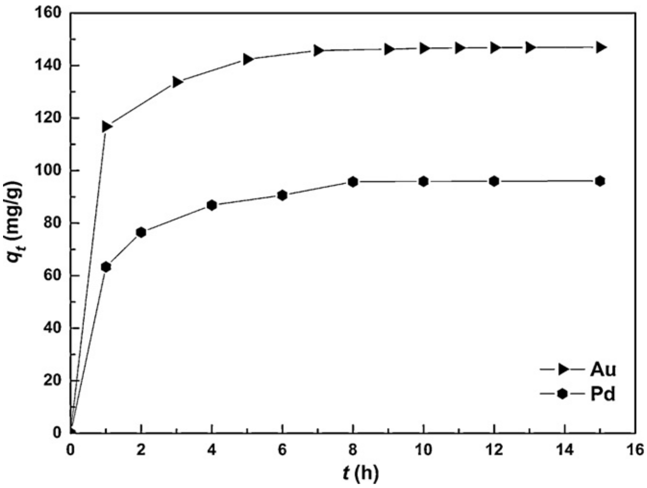

**Fig. 5.** Effect of contact time on the adsorption of Au(III) and Pd(II) by CSGO$_5$ (adsorbent dose: 2 mg; contact time: 20 h; initial concentrations: Au(III) 30 mg/L, Pd(II) 20 mg/L).

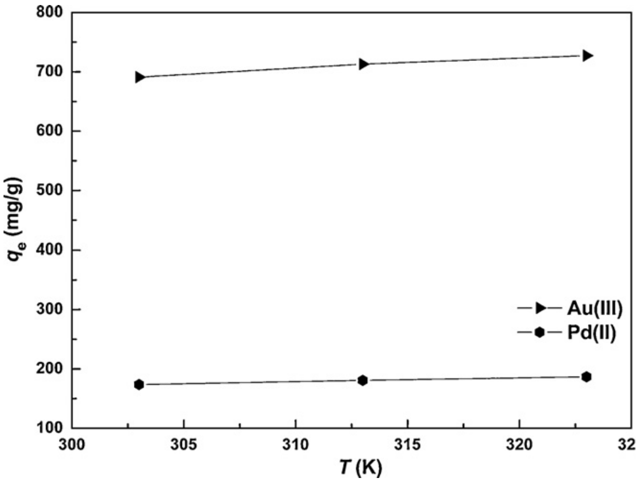

**Fig. 6.** Effect of temperature on the adsorption of Au(III) and Pd (II) by CSGO$_5$ (adsorbent dose: adsorption mass: 2 mg; contact time: 16 h; initial concentrations: Au(III) 150 mg/L, Pd(II) 40 mg/L).

then intraparticle diffusion is not the rate-limiting step and the adsorption mechanism is quite complex.

Fig. 5 shows the kinetic results of Au(III) and Pd(II) adsorbed onto CSGO$_5$. It is observed from Fig. 5 that the adsorption capacity of Au(III) and Pd(II) increased with time. The adsorption rate was high at initial adsorption period of time. This result might due to the availability of large number of vacant sites that saturated with time. The adsorption equilibrium of Au(II) and Pd(II) was attained in 13 h and 12 h, respectively. The pseudo-second-order kinetic parameters and intraparticle diffusion rate constants for the adsorption of Au(III) and Pd(II) on CSGO$_5$ are shown in Table 3. As shown in Table 3, the $R^2$ values of pseudo-second-order model for the adsorption of Au(III) and Pd(II) were 0.9998 and 0.9996 and those of intraparticle diffusion model were 0.7968 and 0.8329, respectively. It is indicated that pseudo-second-order model provided a better correlation in contrast to the intraparticle diffusion model. The $q_e$ values calculated by the pseudo-second-order equation were 150.38 mg/g for Au(III) and 100.60 mg/g for Pd(II), which were close to the values obtained by experiments. The lines of intraparticle diffusion of Au(III) and Pd(II) showed multilinearity with three different adsorption phases. They were (a) the external surface adsorption, (b) the gradual adsorption stage and the intraparticle diffusion is the rate limiting step, and (c) equilibrium stage. Moreover, the lines did not pass through the origin. Hence, the results stated that the chemical adsorption was the rate-limiting step and the adsorption kinetics of Au(III) and Pd(II) on CSGO$_5$ can be well described by the pseudo-second-order model.

### 3.5. Thermodynamic studies

The effect of temperature for the adsorption of Au(III) and Pd(II) on CSGO$_5$ (2 mg) was performed at 303 K, 313 K and 323 K. The initial concentration with desired pH was 150 mg/L and 40 mg/L in case of Au(III) and Pd(II), respectively. And the solutions were shaken for 16 h. The results are shown in Fig. 6. It is apparent that the adsorption capacity increased with the temperature ranging from 303 K to 323 K. The results signified that the process of adsorption was endothermic.

Data from adsorption experiments of the effect of temperature were used to estimate the values of thermodynamic parameters such as Gibbs energy ($\Delta G^\circ$), enthalpy ($\Delta H^\circ$), and entropy ($\Delta S^\circ$), which are determined by the following equations [47]:

$$K_c = \frac{q_e}{C_e} \quad (8)$$

$$\Delta G^\circ = -RT \ln K_c \quad (9)$$

$$\ln K_c = \frac{\Delta S^\circ}{R} - \frac{\Delta H^\circ}{RT} \quad (10)$$

where $R$ (8.3145 J/mol K) is the ideal gas constant, $T$ (K) is the absolute temperature and $K_c$ is the thermodynamic equilibrium constant. The values of $\Delta H^\circ$ and $\Delta S^\circ$ are calculated from the slope

**Table 4**
Thermodynamic parameters for Au(III) and Pd(II) onto CSGO$_5$.

| Metal | Temperature (K) | $\Delta G^\circ$ (kJ/mol) | $\Delta H^\circ$ (kJ/mol) | $\Delta S^\circ$ (J/mol K) | $R^2$ |
|---|---|---|---|---|---|
| Au(III) | 303 | −10.252 | 40.862 | 168.640 | 0.9995 |
| | 313 | −11.887 | | | |
| | 323 | −13.627 | | | |
| Pd(II) | 303 | −8.813 | 30.614 | 130.014 | 0.9962 |
| | 313 | −10.011 | | | |
| | 323 | −11.418 | | | |

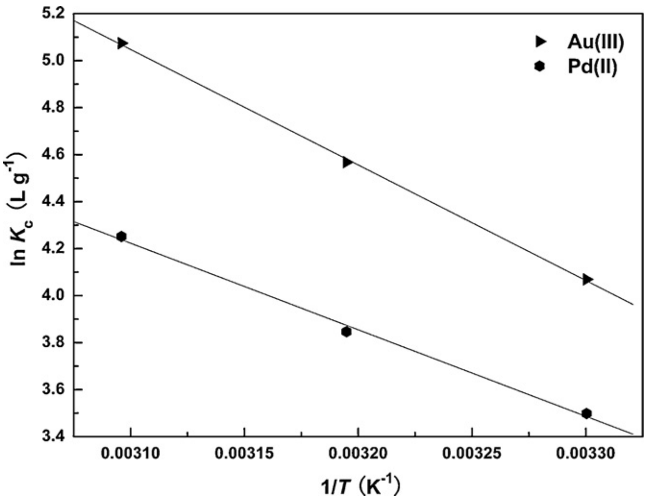

**Fig. 7.** Plot of $\ln K_L$ vs. $1/T$ for adsorption of Au(III) and Pd(II) onto $CSGO_5$.

**Table 5**
Desorption data of Au(III) and Pd (II).

| Desorption agent | Desorption (%) | |
|---|---|---|
| | Au(III) | Pd(II) |
| Thiourea | | |
| 0.3 M Thiourea | 74.98 | 69.18 |
| 0.5 M Thiourea | 70.95 | 87.87 |
| 1.0 M Thiourea | 62.24 | 94.19 |
| 1.5 M Thiourea | 73.34 | 89.70 |
| Thiourea–HCl | | |
| 0.2 M Thiourea–0.5 M HCl | 97.48 | 99.38 |
| 0.5 M Thiourea–0.5 M HCl | 97.57 | 96.54 |
| 1.0 M Thiourea–0.5 M HCl | 99.89 | 89.96 |
| 1.5 M Thiourea–0.5 M HCl | 91.53 | 90.70 |

and intercept of the Van't Hoff linear plots of $\ln K_c$ vs. $1/T$ (shown in Fig. 7) by using Eq. (10). The results are presented in Table 4.

The negative values of $\Delta G^{\circ}$ confirmed the spontaneous nature of the adsorption [48]. As the temperature increased, the negative values of $\Delta G^{\circ}$ increased, indicating more adsorption capacity at higher temperatures. The positive values of $\Delta H^{\circ}$ reflected the endothermic nature of adsorption of both Au(III) and Pd(II) onto $CSGO_5$. The positive values of $\Delta S^{\circ}$ mean an irregular increase of the randomness at the $CSGO_5$/solution interface during the adsorption process.

### 3.6. *Desorption studies and reuse*

In the present study, the desorption percentage of adsorbed Au(III) (initial concentration: 100 mg/L) and Pd(II) (initial concentration: 40 mg/L) onto 2 mg $CSGO_5$ was studied by various concentrations of 10 mL thiourea, HCl and thiourea–HCl solutions at room temperature. Table 5 presents the desorption results. The results showed that the highest desorption percentage reached to nearly 100% in case of Au(III) and 99.38% in case of Pd(II) when 1.0 M thiourea–0.5 M HCl solution and 0.2 M thiourea–0.5 M HCl solution were used as desorption agents, respectively. Table 6 shows the adsorption–desorption cycles of Au(III) and Pd(II) onto $CSGO_5$. It can be found that the desorption amounts were not significantly changed up to 3 cycles and the desorption percentage were above 95%. Hence, the adsorbent $CSGO_5$ can be successfully used for the recovery of Au(III) and Pd(II).

**Table 6**
Adsorption and desorption recycles.

| Cycle | Au(III) | | Pd(II) | |
|---|---|---|---|---|
| | *q* (mg/g) | Desorption (%) | *q* (mg/g) | Desorption (%) |
| 1 | 474.950 | 99.89 | 170.620 | 99.38 |
| 2 | 472.860 | 99.21 | 169.940 | 99.14 |
| 3 | 470.585 | 98.75 | 168.380 | 98.73 |

### 3.7. *Sample analysis*

5.0 mg $CSGO_5$ was employed for the adsorption and elution of standard ore samples, GBW(E)070015 and GBW07293. The obtained amounts of Au(III) and Pd(II) were determined as 8.21 μg/g and 0.499 μg/g, whereas the standard contents were 10.0 μg/g and 0.568 μg/g, respectively. The relative standard deviation ($n = 6$) values were 1.39% and 1.80%, respectively. In addition, the limits of detection (LOD) of Au(III) and Pd(II) were calculated using the IUPAC recommendation which was based on ten times the standard deviation of the peak height. LODs of Au(III) and Pd(II) were 0.013 mg/L and 0.017 mg/L, respectively. The results demonstrated that $CSGO_5$ was able to separate Au(III) and Pd(II) from ore samples, which can be used in mineralogical analysis.

## 4. Conclusions

GO, CSGO composites and GCCS were prepared for the adsorption of Au(III) and Pd(II). The maximum adsorption onto CSGO composites occurred at a wider pH range than that of GCCS. And $CSGO_5$ enhanced the adsorption capacity of Au(III) and Pd(II) compared with GCCS. The experimental data of $CSGO_5$ were well fitted by the Langmuir isotherm models in case of Au(III) and Pd(II). From the Langmuir isotherm data, $CSGO_5$ had the largest adsorption capacity for Au(III) and Pd(II). The pseudo-second-order model provided better correlation of the adsorption data than intraparticle diffusion model, implying that the intraparticle diffusion was not the rate-limiting step. Thermodynamic parameters suggested that the adsorption of Au(III) and Pd(II) onto $CSGO_5$ were spontaneous, endothermic and feasible in nature. The desorption studies showed that 1.0 M thiourea–0.5 M HCl solution and 0.2 M thiourea–0.5 M HCl solution can be effectively used for the adsorption–desorption cycles of Au(III) and Pd(II) onto $CSGO_5$, respectively. Therefore, $CSGO_5$ can enhance the adsorption capacity for Au(III) and Pd(II) and it can be well used for the recovery of Au(III) and Pd(II) in a larger pH range. $CSGO_5$ is a promising adsorbent for the adsorption of Au(III) and Pd(II) in practice.

## References

[1] N. Das, Hydrometallurgy 103 (2010) 180.
[2] M.A. Maheswari, M.S. Subramanian, Talanta 64 (2004) 202.
[3] M. Soylak, M. Tuzen, J. Hazard. Mater. 152 (2008) 656.
[4] M. Soylak, S. Saracoglu, U. Divrikli, L. Elci, Talanta 66 (2005) 1098.
[5] D. Li, X. Chang, Z. Hu, Q. Wang, Z. Tu, R. Li, Microchimi. Acta 174 (2011) 131.
[6] M. Hidalgo, A. Uheida, V. Salvadó, C. Fontàs, Solvent Extr. Ion Exch. 24 (2006) 931.
[7] K. Ihara, S.I. Hasegawa, K. Naito, Talanta 75 (2008) 944.
[8] L. Feng, Y. Zhang, L. Wen, Z. Shen, Y. Guan, Talanta 84 (2011) 913.
[9] X. Feng, Z. Wu, X. Chen, Sep. Purif. Technol. 57 (2007) 257.
[10] X. Chen, K.F. Lam, S.F. Mak, K.L. Yeung, J. Hazard. Mater. 186 (2011) 902.
[11] E. Boyacı, A.E. Eroğlu, T. Shahwan, Talanta 80 (2010) 1452.
[12] Y. Wu, S. Zhang, X. Guo, H. Huang, Bioresour. Technol. 99 (2008) 7709.
[13] X. Guo, S. Zhang, X. Shan, J. Hazard. Mater. 151 (2008) 134.
[14] E. Özdemir, D. Duranoğlu, Ü. Beker, A.Ö. Avcı, Chem. Eng. J. 172 (2011) 207.
[15] P. Daorattanachai, F. Unob, A. Imyim, Talanta 67 (2005) 59.
[16] G. Chakrapani, P.L. Mahanta, D.S.R. Murty, B. Gomathy, Tanlanta 53 (2001) 1139.
[17] J.N. Petersen, B.H. Davison, C.D. Scott, S.L. Blankinship, Biotechnol. Bioeng. 38 (1991) 923.
[18] C.M. Hasfalina, R.Z. Maryam, C.A. Luqman, M. Rashid, J. Nat. Fibers 7 (2010) 267.
[19] E. Guibal, Sep. Purif. Technol. 38 (2004) 43.
[20] M.L.P. Dalida, A.F.V. Mariano, C.M. Futalan, C.C. Kan, W.C. Tsai, M.W. Wan, Desalination 275 (2011) 154.
[21] M.M. Lou, B. Zhu, I. Muhammad, B. Li, G.L. Xie, Y.L. Wang, H.Y. Li, G.C. Sun, Carbohyd. Res. 346 (2011) 1294.

[22] R.R. Araiza, P. Alcouffe, C. Rochas, A. Montembault, L. David, Langmuir 26 (2010) 17495.
[23] H. Sashiwa, S. Aiba, Prog. Polym. Sci. 29 (2004) 887.
[24] S.H. Lim, S.M. Hudson, Color Technol. 120 (2004).
[25] J.H. Park, G. Saravanakumar, K. Kim, I.C. Kwon, Adv. Drug Deliv. Rev. 62 (2010) 28.
[26] K.Z. Elwakeel, J. Dispersion Sci. Technol. 31 (2010) 273.
[27] F. Li, C. Bao, J. Zhang, Q. Sun, W. Kong, X. Han, Y. Wang, J. Appl. Polym. Sci. 113 (2009) 1604.
[28] A.M. Donia, A. Atia, K.Z. Elwakeel, Hydrometallurgy 87 (2007) 197.
[29] S. Kushwaha, P.P. Sudhakar, Carbohydr. Polym. 86 (2011) 1055.
[30] E.S. Dragan, M.V. Dinu, D. Timpu, Bioresour. Technol. 101 (2010) 812.
[31] B. Wang, Y. Chang, L. Zhi, New Carbon Mater. 26 (2011) 31.
[32] C.G. Navarro, M. Burghard, K. Kern, Nano Lett. 8 (2008) 2045.
[33] D. Eom, D. Prezzi, K.T. Rim, H. Zhou, M. Lefenfeld, S. Xiao, C. Nuckolls, M.S. Hybertsen, T.F. Heinz, G.W. Flynn, Nano Lett. 9 (2009) 2844.
[34] Y.R. Tzeng, W.W. Pai, C.S. Tsao, M.S. Yu, J. Phys. Chem. C 115 (2011) 12023.
[35] X. Zhao, N. Song, Q. Jia, W. Zhou, Microchim. Acta 166 (2009) 329.
[36] W.S. Hummers Jr., R.E. Offeman, J. Am. Chem. Soc. 80 (1958) 1339.
[37] H.A. Becerril, J. Mao, Z. Liu, R.M. Stoltenberg, Z. Bao, Y. Chen, ACS Nano 2 (2008) 463.
[38] W. Zhang, C. Zhou, W. Zhou, A. Lei, Q. Zhang, Q. Wan, B. Zou, Environ. Contam. Tox. 87 (2011) 86.
[39] X. Yang, Y. Tu, L. Li, S. Shang, X. Tao, ACS Appl. Mater. Int. 2 (2010) 1707.
[40] P. Sorlier, A. Denuzière, C. Viton, A. Domard, Biomacromolecules 2 (2001) 765.
[41] I. Langmuir, J. Am. Chem. Soc. 40 (1918) 1361.
[42] H. Freundlich, Z. Phys. Chem. 57 (1906) 387.
[43] Y.S. Ho, G. McKay, Process Biochem. 34 (1999) 451.
[44] F.M. Oliveira, B.F. Somera, M.Z. Corazza, M.J.S. Yabe, M.G. Segatelli, E.S. Ribeiro, É.C. Lima, S.L.P. Dias, C.R.T. Tarley, Talanta 85 (2011) 2417.
[45] W.J. Weber, J.C. Morris, J. Sanit. Eng. Div. Am. Soc. Civ. Eng. 89 (1963) 31.
[46] M.S.E. Shahawi, M.A.E. Sonbati, Talanta 67 (2005) 806.
[47] N. Tewari, P. Vasudevan, B. Guha, Biochem. Eng. J. 23 (2005) 185.
[48] M.V. Subbaiah, Y. Vijaya, A.S. Reddy, G. Yuvaraja, A. Krishnaiah, Desalination 276 (2011) 310.